

Reconsider the shear paradigm - stirring and aeration strategies in cell culture processes

Florian Strobl

Austrian Centre of Industrial Biotechnology (Austria)

Mark Dürkop

Novasign GmbH

Dieter Palmberger

Austrian Centre of Industrial Biotechnology (Austria)

Gerald Striedner (✉ Gerald.Striedner@boku.ac.at)

University of Natural Resources and Life Sciences

Research Article

Keywords: cell culture processes, continuously stirred tank reactors (CSTRs), aeration strategies

Posted Date: December 11th, 2020

DOI: <https://doi.org/10.21203/rs.3.rs-122078/v1>

License: © ⓘ This work is licensed under a Creative Commons Attribution 4.0 International License.

[Read Full License](#)

Abstract

Multicellular organisms cultivated in continuously stirred tank reactors (CSTRs), are more sensitive to the environmental conditions prevalent in suspension culture than to bacteria. Stirring, mandatory for efficiently providing oxygen and simultaneously preventing concentration gradients, is a major shear source. The primary approach for reducing shear-associated cell damage is to employ unique impeller designs, combined with slow stirring speeds, to maintain efficient mixing and aeration. Here, we characterized the shear resistance of insect and CHO cells in suspension. We applied a microfluidic device that allows defined variations in shear rates, and both cell lines displayed resistance to shear rates up to $8.73 \times 10^5 \text{ s}^{-1}$. The unexpectedly high shear resistance of these cells made it possible to design new cultivation strategies, diametric to state-of-the-art strategies. We applied Rushton turbine-powered CSTRs, typically employed in microbial processes, to both cell cultures, at high revolution speeds and low aeration rates. With this strategy, we significantly reduced aeration and foam formation, and it was no longer necessary to add pure oxygen to ensure efficient aeration. This novel cultivation approach can eliminate a number of existing bottlenecks in state-of-the-art cell culture processes and provide a wide range of possibilities for developing highly efficient, robust next generation cell culture processes.

Introduction

In the biopharmaceutical industry, products are mainly produced by cultivating organisms in suspension. A rather small share (only 2.3%) of all newly approved active pharmaceutical ingredients (APIs) are produced with insect cells as host. Insect cells produce recombinant proteins and virus-like particles (VLPs), a highly complex product class that is rapidly gaining importance [1]. In contrast, Chinese hamster ovary cells (CHOs) are the main work-horse in biopharmaceutical production; they produced 51% of all newly approved APIs from 2014 to 2018 [2]. Based on fermentation technologies and operating strategies developed for CHOs, a broad portfolio of methodologies is available, which can be transferred to insect cell processes with only minor modifications. The system of choice for cultivating these cell types in suspension is the continuous stirred tank reactor (CSTR). CSTRs can be either stainless steel, multi-use bioreactors, with up to 25 m^3 of working volume [3], or a single-use bioreactor with up to 2 m^3 of working volume [4].

The main relevant difference between processing mammalian cell lines and processing insect cell lines is the specific oxygen demand. Compared to mammalian cell lines, *Spodoptera frugiperda* (Sf9) cells require four times higher specific oxygen and *Hi-5* (*Trichoplusia Ni*) insect cells require 13 times higher specific oxygen [5], and this demand increases by 30–40% after the culture is infected [6, 7]. Thus, the main challenge in cultivating insect cells is to overcome the interfering problems of high oxygen demand and high shear sensitivity. Moreover, both these problems become more pronounced in the production phase, after the cells are infected.

The key process parameter is the oxygen transfer rate (OTR). The OTR can be influenced during the cultivation process by the stirring speed, air flow rate, partial pressure of oxygen, head space pressure,

fermentation broth temperature, and media composition [8]. The challenge is to ensure efficient transfer of the oxygen required for cell growth and production, and simultaneously, to maintain low shear rates to prevent cell disruption. However, although the stirring speed and the air flow rate are key process inputs for varying the OTR, they are also mainly responsible for increasing shear in the bioreactor. Consequently, the general state-of-the-art practice with CSTRs in insect cell cultures is to reduce the stirring speed to a level that fulfills mixing requirements and to manipulate oxygen transfer, via the flow rate and the composition of the supplied gas. CSTRs for cultivating mammalian and insect cell lines are designed, in particular, to maintain low shear forces caused by stirring. The typical height to diameter (H/D) ratios for mammalian cell culture bioreactors are in the range of 1.5–2:1 [9]; the standard gas transfer coefficient, $k_L a$, ranges from 5–10 h^{-1} ; and the specific power input ranges from 5 to 300 W m^{-3} [10]. However, increasing the gas flow causes foam formation, and bursting air bubbles on the liquid surface increase the shear; both these effects contribute to the destruction of cells and VLPs [11],[12]. Conversely, low stirring speeds and thus, limited mixing efficiency, can amplify the problem of zone and gradient formation [13], at least at larger scales, which can cause additional cellular stress [14].

Due to the lack of methods for determining cellular shear sensitivity, little or no objective data are available on insect cells. Moreover, existing knowledge is largely based on empirical data and experience with similar cell types. To address the shear sensitivity of cells, we applied a microfluidic shear device [15] that could quantify the shear resistances of insect and CHO cells under controlled conditions. We applied a range of shear rates to insect cells to determine the tolerable range of shear for these cell types.

Based on those results, in the present study, we aimed to develop a new cell cultivation strategy with high stirring speeds that enabled efficient oxygen transfer, efficient mixing, and low aeration rates to reduce shear forces triggered by bubble ruptures and foam formation. We used microbial CSTRs, which differ dramatically from cell culture reactors, in terms of reactor geometry (H/D ratios: 2.5–3:1 or more), oxygen transfer capacity ($k_L a > 250 \text{ h}^{-1}$, and may exceed 1000 h^{-1} [16, 17]), and specific power input ($\approx 5 \text{ kWx m}^3$ [18], [19], [20]). We hypothesized that this new process operation would maintain optimal production/growth conditions up to high cell densities without requiring pure oxygen, would reduce foam formation, and would shorten the mixing times for efficient infections.

Materials And Methods

Cell lines

We purchased two High Five™ (ThermoFisher) insect cell lines: the BTI-TN-5B1-4 cell line and the Tnms42 (TN42) cell line (BTI, Gary W. Blissard), which was an alpha-nodavirus-free, TN-5B1-4 derivative [21]. In addition, we acquired a host cell variant of CHO-K1 (ATCC CCL-61) that was adapted to serum-free medium [22] (Antibody Lab GmbH, Vienna, Austria). The stable CHO-K1/D1 clonal cell line produced an IgG1 antibody that specifically recognized tumor necrosis factor alpha.

Cloning and generating recombinant baculoviruses and the virus stock

We used a baculovirus that encoded the hemagglutinin (HA) protein of Influenza virus A/California/04/2009 (H1N1) (GenBank accession no. JF915184.1) and the matrix protein for the Gag-polyprotein (Gag) of type 1 human immunodeficiency virus (GenBank accession no. K03455.1). These recombinant genes were codon-optimized for expression in *Trichoplusia ni* (IDTdna, Leuven, Belgium). After PCR amplification, the HA of H1N1 was inserted into the pACEBac-1 acceptor vector (EMBL, Grenoble), which resulted in pACEBac-1-H1. Similarly, the Gag fragment was cloned into the pIDC donor vector (EMBL, Grenoble), which resulted in pIDC-Gag. A Cre-LoxP recombination of the acceptor and donor vectors resulted in H1-Gag acceptor-donor fusion plasmids. The H1-Gag fusion plasmid was transformed into either *E. coli* DH10EMBacY (EMBL, Grenoble) or DH10EMBacp6.9Y cells, which harbored a yellow fluorescent protein (YFP) expression cassette under the control of the polH or p6.9 promoter, respectively. The purified bacmid DNA was transfected into *Sf9* cells with the FuGene HD transfection reagent (Promega, Madison, Wisconsin, USA) according to the manufacturer's instructions. Viral titers were raised by subsequent passaging, and the titer of the passage 3 stock was determined by measuring the half-maximal tissue culture infective dose (TCID₅₀).

Shear experiments

The shear sensitivity and resistance of cells in suspension were tested with a shear device developed by Dürkop et al. [23]. This device was a T-4-SS micro-orifice (O'Keefe Control Co., Monroe, CT, USA) with a 15-fold reduction in diameter (from 1/16" to 99 μm). It previously generated shear rates up to 10⁸ s⁻¹ when used to evaluate the shear sensitivity of proteins [23]. We modified the described method by using a Nemesys XL syringe pump (Cetoni GmbH, Korbussen, Germany), instead of an ÄKTA P100 piston pump, to reduce cell stress inside the pump. Figure 1 illustrates the experimental set-up. With a two-way valve (3), the cells could either be pumped from the sample reservoir (1) into the syringe pump (2) or, when the valve was switched, cells were pumped from the syringe pump (2) through an orifice (4), and into the sample collector (5).

Cells were pumped through the orifice at different volume flow rates. By increasing the volumetric flow rate, the shear rate was increased. We calculated the average and maximum shear rates (γ), as follows:

$$\gamma_{average} = \frac{16v}{3d} \quad (1)$$

$$\gamma_{max} = \frac{8v}{d} \quad (2),$$

where v is the velocity [m/s], and d is the diameter of the orifice [m]. Equations (1) and (2) are only valid in laminar flow conditions, which were applied in these experiments. In addition, the collected cells were counted, and viability was determined.

Shake flask cultivations

Insect cell cultivation

For each experiment, cells from adherent cultures were transferred to suspension at a starting concentration of 0.5×10^6 cells/mL. Cells were then expanded to the required cell concentrations. For all experiments, the cells were maintained in the exponential growth phase at 27°C in shaker flasks, agitated at 100 rpm, and passaged until they reached a cell concentration of 4×10^6 cells/mL. Then, cells were grown in serum-free medium (Hyclone SFM4Insect, GE Healthcare). Viable cell counts (VCC) were determined with the trypan blue stain method in an automated cell counter (TC20 Biorad).

CHO cell cultivation

To acquire the seed culture, cells were thawed from a working cell bank and cultured in Dynamis AGT Medium (A26175-01, Thermo Fisher Scientific, USA), supplemented with 8 mM L-Glutamine (25030081, Sigma-Aldrich, USA), 1:1000 Anti-Clumping Agent (01-0057AE, Thermo Fisher Scientific) and 0.7 mg/L G418 (108321-42-2, Thermo Fisher Scientific). For pre-cultures, cells were sub-cultured in Dynamis AGT Medium with 8 mM L-Glutamine every 3 to 4 days at 37°C, in a humidified incubator (Heracell v10S 160, Thermo Fisher Scientific) with 5% v/v CO₂, and agitated at 200 rpm on an orbital shaker (88881102, Thermo Fisher Scientific). Cells were diluted to a total cell count (TCC) of 1.5×10^6 cells/mL in Dynamis AGT Medium before the shear stress tests.

Bioreactor cultivation

Experiments were performed in 1 L (BioFlo320 1L, Eppendorf) and 1.5 L (DASGIP SR1500 DLS, Eppendorf) bioreactors. The BioFlo320 bioreactor system was equipped with one pitched-blade impeller (3 blades; 45°). The DASGIP bioreactor system was equipped with a six-blade Rushton impeller.

The BioFlo320 system maintained the dissolved oxygen level at 30%, and pure oxygen was supplemented when needed. The temperature was maintained at 27 °C, and the pH was monitored. This setup was chosen, because it was described previously [6], [24]. The 1.5 L DASGIP bioreactor maintained the pH at 6.4 ± 0.05 with 25% phosphoric acid and 7.5% sodium bicarbonate.

Bioreactor infection strategy

Cells were grown in the bioreactor in batch mode, until they reached a cell density of about 2×10^6 cells/mL. Next, they were infected with the generated baculovirus stock, at a multiplicity of infection (MOI) of 1 and diluted with fresh media to a final density of 1×10^6 cells/mL.

Analytical methods: Tissue culture infectious dose assay

The titer of virus stocks was determined by measuring the TCID₅₀ [25], based on the detection of YFP fluorescence. Briefly, *Sf9* cells were infected with serial dilutions of virus stock or supernatant samples of the different cultivations in a 96-well culture plate (Corning Incorporated, USA). Plates were incubated at 27°C without agitation. After 4 days, the wells were inspected with a fluorescence microscope (Leica DMIL-LED).

Results And Discussion

Shear resistance of cell-lines: shear device experiments

To evaluate the influence of shear on insect and CHO cell lines, we set up controlled shear conditions with a micro-fluid shear device. In the first step, we conducted a control experiment to test the influence of the syringe pump and tubing on cell viability. We filled the syringe pump with the cell suspension and pumped it through the flow path without the nozzle. These experiments were performed at maximum pump speed (45 mL/min), which was the speed used to fill the syringe pump with the cell suspension. We evaluated cell viability before and after this treatment.

Next, directly before each experiment, we prepared 50-mL batches of cell suspensions at cell concentrations of 1.5×10^6 cells/mL. We used an untreated cell suspension with a defined cell concentration and viability as the reference sample (control). Then, a 20-mL aliquot of suspended cells was drawn into the syringe pump each passage and pumped through the device. The first 10-mL fraction of cells was discarded to exclude potential impurities from a former run. The fraction from 10 to 15 mL was used to evaluate cell viability. Each volume flow rate was measured in triplicate, if not otherwise indicated, and the system was flushed with media between volume flow rate changes. We selected three different volume flow rates (3, 5, and 10 mL/min) for shear rate determinations (Table 1). For all the tested flow conditions, a laminar flow profile was present inside the shear device; thus, we used Equations (1) and (2) for shear determinations. We also calculated the dimensionless shear, which was the product of the average shear rate and the incubation time. For proteins, it was assumed that, when the dimensionless shear exceeded 10^4 , the proteins would irreversibly aggregate [26]. Although this theory was previously shown to be false for a large set of proteins [15], the result could be true for cells.

Table 1

Flow rates inside the shear device, with corresponding Reynolds number, maximum and average shear rates, and the dimensionless shear

flow rate [mL/min]	Reynolds number	max shear rate [s^{-1}]	average shear rate [s^{-1}]	dimensionless shear
3	613.47	5.24E + 05	3.49E + 05	17.93
5	1022.45	8.73E + 05	5.82E + 05	17.93
10	2044.89	1.75E + 06	1.16E + 06	17.93

Furthermore, we showed that dimensionless shear-associated aggregation did not apply to these cells. The product of incubation time and shear rate was constant inside the shear device, because at higher flow rates, the incubation time was reduced by the same amount as the shear rate was increased. Hence, the dimensionless shear was constant, as long as the flow conditions remained laminar. However, at higher flow rates, the viability decreased. This decrease indicated that cell damage occurred when the shear rate exceeded the threshold that maintained a constant dimensionless shear.

Our experiments, conducted under controlled shear conditions, indicated that all three cell lines could withstand much higher shear rates than expected, based on the literature [27]. Figure 2 shows that all cell lines could withstand flow rates up to 5 mL/min, which imposed maximum and average shear rates of up to $8.73 \times 10^5 \text{ s}^{-1}$ and $5.82 \times 10^5 \text{ s}^{-1}$, respectively (Table 1). The increase in the TCC at flow rates of 3 and 5 mL/min could be attributed to the dispersion of cell clumps when passing through the orifice of the shear device. However, the shear imposed by 10-mL/min flow rates reduced the TCC and VCC. In addition, we observed a sharp increase in the VCC/TCC ratio. This finding indicated that some cells could not withstand a single passage, when the maximum shear was $> 8.73 \times 10^5 \text{ s}^{-1}$ and the average shear was $> 5.82 \times 10^5 \text{ s}^{-1}$. However, at lower shear rates, the shear had a positive effect, due to the dispersion of cell clumps; clump dispersion also occurs when cells are filtered [28].

Bioreactor shear characterization

In a theoretical analysis, Sánchez Pérez and Rodríguez Porcel [29] established the connection between the average shear rate (γ_{av}) and the rotational speed of the impeller in turbulent flow. Below, Equation (3) is based on a simplified assumption correlated to empirical data. In Equation (4), the maximum shear stress (γ_{max}) also took into account the media and type of impeller used.

The relationship between the stirring speed (N) in a CSTR and the average shear rate (γ_{av}) [29], for an A315 axial flow hydrofoil impeller, was:

$$\gamma_{av} = 33.1 \times N^{1.4} \quad (3)$$

The relationship between the stirring speed (N) in a CSTR and the maximum shear stress (γ_{max}) [30] was:

$$\gamma_{max} = 3.3 \times N^{1.5} \times d_i \left(\frac{\rho}{\mu} \right)^{0.5} \quad (4),$$

where $\mu = 1.1 \text{ mPas}$, $\rho = 1050 \text{ kg/m}^3$ are related to the used media, and $d_i = 0.06\text{m}$ of the used Rushton impeller.

The calculated average and maximum shears, based on Equations (3) and (4) are shown in Table 2 for reasonable stirrer speeds that are typically used in bench-top bioreactors. According to these numbers, any stirring speed currently used in bioreactors would be below the critical value for the cell lines tested with the shear device. Consequently, shear generated in a bioreactor equipped with a stirrer and one pitched-blade impeller should never exceed the critical limit for insect cells.

Table 2

Stirring speeds and corresponding average (γ_{av}) and maximum (γ_{max}) shear rates for a 1 L bioreactor equipped with one pitched-blade impeller

Speed, rpm	γ_{av} [s^{-1}] ^a	γ_{max} [s^{-1}]	dimensionless shear
100	6.77E + 01	4.16E + 02	2.34E + 07
200	1.79E + 02	1.18E + 03	6.17E + 07
500	6.44E + 02	4.65E + 03	2.23E + 08
800	1.24E + 03	9.42E + 03	4.30E + 08
1000	1.70E + 03	1.32E + 04	5.87E + 08
1500	3.00E + 03	2.42E + 04	1.04E + 09

^aThe average shear values were generated by Sánchez Pérez and Rodríguez Porcel [29] with Eq. 4, for an A315 axial flow hydrofoil impeller (LIGHTNIN Mixers, Rochester, NY), which is similar to a pitched-blade stirrer.

Furthermore, when a cell cultivation lasts 96 h, the dimensionless shear would be up to 8 orders of magnitude above the shear observed in the shear device. This highlights the assumption that, if proteins are incubated for a very long time, they could be harmed even by low shear rates. If we assumed that cells behaved like proteins, then cells incubated for long times should experience viability problems, even at very low stirring speeds. However, our findings indicated that cells were less shear-sensitive than previously reported. We found that the maximum shear rate for short periods of time damaged cells, but an average shear rate for an extended period of time did not damage cells.

Bioreactor Shear experiments

The experiments with the shear device and the estimation of shear rates inside the bioreactor led to our conclusion that shear generated by stirring was not likely to damage insect cells. Because both insect cell lines showed similar behavior, we selected the TN42 cell line for the next series of experiments, which focused on verification of the shear device results.

In the first step, we conducted a TN42 reference cultivation, run under standard operation conditions, in a 1 L BioFlo320 System (Eppendorf) equipped with one pitched-blade impeller. This experiment generated reference process data (Fig. 3).

In this reference experiment, cells were seeded at 0.5×10^6 cells/mL and grown in batch mode until they reached 2×10^6 cells/mL. At this point, the cells were infected with the baculovirus working virus stock at a MOI of 1, and they were diluted with fresh medium to 1.0×10^6 cells/mL (Fig. 3A). The stirring speed ranged from 100 to 160 rpm, and the aeration rate ranged from 0.2 to 0.5 standard liter per minute (SLPM). The results showed that, even at a cell concentration of 1.5×10^6 cells/mL, after infection, it was

necessary to add pure oxygen to maintain the dissolved oxygen level at 30% and avoid high stirring rates. Infection caused a decline in the cell growth rate, and at 48 h post infection, cell viability was reduced to 91.4% (Fig. 3A).

According to Table 2, the shear in the reference setting was more than two orders of magnitude below the critical values determined in the microfluidic shear device experiments. Therefore, to introduce higher shear rates with stirring, we switched to a microbial bioreactor (SR1500DLS, Eppendorf DASGIP System) equipped with one Rushton impeller. Cells were grown in a 500 mL batch volume and the stirring speed was set to 200 rpm, as a starting value. The air flow was maintained at a constant 0.016 SLPM. Cells were seeded at 0.5×10^6 cells/mL and grown in batch mode for 72 h without the addition of fresh media. The cell viability increased during the batch run, and the cell density reached 4.5×10^6 cells/mL (Fig. 4A). Cell viability was not impacted by the shear rates generated with a Rushton impeller, even running at speeds up to 270 rpm.

The next cultivation was performed at a working volume of 1L, but the reactor was equipped with three Rushton blades. The batch cultivation (Fig. 4C) was started at 400 rpm, and a step increase to 800 rpm was applied after 48 h of cultivation. The aeration rate was set to 0.016 SPLM to minimize bubbles and foam formation, because no antifoam was used in this experiment. Although the inoculated cells showed low viability compared to the other batches (Fig. 4A), their viability increased in the first 48 h, from 79.6–82%. This increase in viability was also observed in the previous experiment (Fig. 4A), which led to the conclusion that a bioreactor powered by a Rushton turbine at 400 rpm would not impact the viability of insect cells. At the initial 400 rpm stirring rate and the low aeration rate, the DO level slowly decreased from 100–65% over the initial 48 h, and the culture reached a cell density of 4.0×10^6 cells/mL during this time. At 48 h, the stirring speed was increased to 800 rpm, and unintentionally, the aeration rate was set to 0 SPLM for the last 24 h of the batch run. Consequently, the DO steadily decreased to 0% for the last couple of hours of the experiment, and cells started to die, due to limited oxygen.

In the next experiment (Fig. 4E,F), the initial stirring speed of 400 rpm was stepped to 1000 rpm at 24 h. At 24 h after this change, the viability initially decreased by about 5%; but at 48 h after the step to 1000 rpm, the viability dropped by 71.5%. This observation can be explained by the high stirring speed, which led to the formation of a liquid vortex, because no baffles were installed in the bioreactor. As a result, additional air was introduced into the suspension via the vortex surface, and the air was split into small bubbles by the Rushton elements. Thus, the shear forces increased, due to bubbles bursting. The cells could not withstand these harsh conditions. Similar observations were previously described by Murhammer and Goochee [31] and by Maranga et al. [32].

New control strategy for insect cell cultivation processes

With the information generated in the preceding experiments, we set up a new DO control strategy in the microbial bioreactor. The goal was to maintain the gas flow rate as low as possible to minimize foam formation and bubble-associated shear. The PID control strategy for maintaining the DO was adapted by

linking the stirring speed, which was the main parameter, to the airflow rate. In the initial phase, the impeller speed was set to the minimum (150 rpm). Then, when the DO level reached the set point of 30%, the controller was set to increase the stirring speed, incrementally, up to a maximum of 800 rpm. The stirrer was equipped with a Rushton impeller, and an L-sparger was used to distribute the aeration gas. During the cultivation of uninfected cells, the stirring speed increased to 300 rpm, and at the end of the exponential growth phase, the TCC was 6×10^6 cells/mL (Fig. 5A). The gas flow rate was set to the minimum of 0.03 SLPM, but unfortunately, the controller could not maintain this precise rate (Fig. 5B,D).

In parallel, the same process control strategy was tested in a batch that received a virus infection at 24 h. Due to the infection and VLP production, cell growth stopped (Fig. 5C), but oxygen consumption continued to increase (Fig. 5D). Additionally, at the timepoint of infection, the aeration rate increased to 0.06 SLPM. Compared to the reference process for the infected batch (Fig. 3), in this set-up, there was no need to add pure oxygen, because increasing the stirring speed provided efficient oxygen transfer.

CHO cultivations

To determine the impact of high shear due to increased stirring speeds, we performed a direct comparison between two CHO batches cultivated at different stirring speeds in a 1.5 L microbial CSTR bioreactor (SR1500DLS, Eppendorf). One bioreactor (Fig. 6A,B) was operated at a low stirring speed, starting at 100 rpm, and the aeration rate was set to 0.03 SLPM. The DO was maintained at 30% by incrementally increasing the stirring speed, which mimicked a standard CHO batch cultivation. The second bioreactor was operated at an increased stirring speed. After a short adjustment phase at 200 rpm, the stirring was maintained at 300 rpm with an aeration rate of 0.03 SLPM. Then, after 48 h, the stirring was increased to 600 rpm, and the aeration rate was lowered to 0.016 SLPM (Fig. 6D). In both reactors, the sparger supplemented the medium with carbon dioxide to control the pH.

We found that cell growth rates behaved nearly the same at the low and high stirring settings (Fig. 6A,C). Moreover, viability was not influenced by the high stirrer speed during exponential growth, which ended at around 96 h after inoculation. At the high stirring speed, the DO never dropped below 80% throughout the entire process (Fig. 6D). However, we observed a difference in viability during the stationary phase; the viability decreased more rapidly in the bioreactor with the faster stirring speed (Fig. 6C,D) than in the bioreactor with the slower speed (Fig. 6A,B).

Overall, our results showed that CHO cells could be cultivated at higher stirring speeds, in combination with a Rushton impeller, without damaging the cells. Additionally, aeration rates could be maintained at a minimum, and it was not necessary to add pure oxygen throughout the process. With the higher stirring rate and the lower aeration rate, foaming was nearly eliminated during the batch cultivations; thus, no antifoam had to be added. Utilizing this new DO control strategy could enable CHO cell cultivations to achieve higher cell concentrations.

Conclusion

The shear device described in this study was an efficient tool for directly applying defined, low to high shear levels to cells and for characterizing cell shear sensitivity. In this study, we used the shear device with insect and CHO cells, but it can also be used for other cell lines, viruses, or VLPs to determine critical shear stress.

We found that both insect cell lines and the CHO cell line could withstand unexpectedly high maximum and average shears of $8.73 \times 10^5 \text{ s}^{-1}$ and $5.82 \times 10^5 \text{ s}^{-1}$, respectively.

Knowledge of the critical shear for the cell types investigated facilitated the design of a new DO process control regime, based on high energy input through stirring, with a Rushton powered microbial bioreactor system. With this system, the oxygen transfer rate could be significantly increased, even at low gas flow rates. As expected from the micro-fluidic experiments, high stirring speeds did not harm either the insect cells or the CHO cells, as long as the gas flow rate and bubble introduction were maintained at low levels. In addition, low aeration rates provided significantly reduced foam formation, which was beneficial for both the process and the cells. The cell densities achieved in this study required maximum stirring speeds of 300 rpm for insect cells and 220 rpm for CHO cells. These stirrer speeds introduced shear rates that were far below the critical values. The reduced cell viability observed in the experiment with a 1000 rpm stirring speed was probably caused by vortex formation, which can simply be prevented by introducing baffles. Our results showed that the oxygen transfer rates that we achieved with this mode of bioreactor operation produced much higher cell densities than were achieved with the standard mode, without the need to increase the gas flow rate or add pure oxygen.

Our new control regime has the advantage of improving the economic efficiency of the process, but more importantly, the lower gas volumes in the suspension also reduced foam formation and bubble rupture at the liquid surface. This phenomenon can affect cell viability, virus quality, and products, like for instance, VLPs.

References

1. Langer, E. and R. Rader, *Biopharmaceutical Manufacturing: Historical and Future Trends in Titters, Yields, and Efficiency in Commercial-Scale Bioprocessing*. BioProcessing Journal, 2015. **13**(4): p. 47-54.
2. Walsh, G., *Biopharmaceutical benchmarks 2018*. Nature Biotechnology, 2018. **36**(12): p. 1136-1145.
3. Farid, S.S., *Process economics of industrial monoclonal antibody manufacture*. J Chromatogr B Analyt Technol Biomed Life Sci, 2007. **848**(1): p. 8-18.
4. Löffelholz, C., et al., *Bioengineering Parameters for Single-Use Bioreactors: Overview and Evaluation of Suitable Methods*. Chemie Ingenieur Technik, 2013. **85**(1-2): p. 40-56.
5. Wagner, B.A., S. Venkataraman, and G.R. Buettner, *The rate of oxygen utilization by cells*. Free radical biology & medicine, 2011. **51**(3): p. 700-712.

6. Kamen, A.A., et al., *Culture of insect cells in helical ribbon impeller bioreactor*. Biotechnol Bioeng, 1991. **38**(6): p. 619-28.
7. Wong, T.K.K., et al., *Relationship between oxygen uptake rate and time of infection of Sf9 insect cells infected with a recombinant baculovirus*. Cytotechnology, 1994. **15**(1): p. 157-167.
8. Garcia-Ochoa, F. and E. Gomez, *Bioreactor scale-up and oxygen transfer rate in microbial processes: An overview*. Biotechnology Advances, 2009. **27**(2): p. 153-176.
9. Godoy-Silva, R., C. Berdugo, and J.J. Chalmers, *Aeration, Mixing, and Hydrodynamics, Animal Cell Bioreactors*. Encyclopedia of Industrial Biotechnology, 2010: p. 1-27.
10. Eisenkraetzer, D., *6.1 Bioreactors for Animal Cell Culture*, in *Animal Cell Biotechnology In Biologics Production*. 2014.
11. Walls, P.L.L., et al., *Quantifying the potential for bursting bubbles to damage suspended cells*. Scientific Reports, 2017. **7**(1): p. 15102.
12. Puente-Massaguer, E., et al., *PEI-Mediated Transient Transfection of High Five Cells at Bioreactor Scale for HIV-1 VLP Production*. Nanomaterials, 2020. **10**(8): p. 1580.
13. Tramper, J., *Oxygen gradients in animal-cell bioreactors*. Cytotechnology, 1995. **18**(1): p. 27-34.
14. Paul, K. and C. Herwig, *Scale-down simulators for mammalian cell culture as tools to access the impact of inhomogeneities occurring in large-scale bioreactors*. Engineering in Life Sciences, 2020. **20**(5-6): p. 197-204.
15. Duerkop, M., et al., *Influence of cavitation and high shear stress on HSA aggregation behavior*. Engineering in Life Sciences, 2018. **18**(3): p. 169-178.
16. Czermak, P., R. Pörtner, and A. Brix, *Special Engineering Aspects*, in *Cell and Tissue Reaction Engineering: With a Contribution by Martin Fussenegger and Wilfried Weber*, R. Eibl, et al., Editors. 2009, Springer Berlin Heidelberg: Berlin, Heidelberg. p. 83-172.
17. Garcia-Ochoa, F., et al., *Oxygen uptake rate in microbial processes: An overview*. Biochemical Engineering Journal, 2010. **49**(3): p. 289-307.
18. Langheinrich, C., et al., *Oxygen Transfer in Stirred Bioreactors Under Animal Cell Culture Conditions*. Food and Bioproducts Processing, 2002. **80**(1): p. 39-44.
19. Sagmeister, P., et al., *Bacterial Suspension Cultures*. Industrial Scale Suspension Culture of Living Cells, 2014: p. 40-93.
20. Jossen, V., et al., *7 - Stirred Bioreactors: Current State and Developments, With Special Emphasis on Biopharmaceutical Production Processes*, in *Current Developments in Biotechnology and Bioengineering*, C. Larroche, et al., Editors. 2017, Elsevier. p. 179-215.
21. Granados, R., Blissard, G., Debbie, P., *Cell Lines That Are Free of Viral Infection and Methods for Their Production*. Google patents. Google Scholar, 2016.
22. Zboray, K., et al., *Heterologous protein production using euchromatin-containing expression vectors in mammalian cells*. Nucleic acids research, 2015. **43**(16): p. e102-e102.

23. Duerkop, M., et al., *Impact of Cavitation, High Shear Stress and Air/Liquid Interfaces on Protein Aggregation*. Biotechnol J, 2018.
24. Zeiser, A., et al., *On-Line Monitoring of Physiological Parameters of Insect Cell Cultures during the Growth and Infection Process*. Biotechnology Progress, 2000. **16**(5): p. 803-808.
25. Smither, S.J., et al., *Comparison of the plaque assay and 50% tissue culture infectious dose assay as methods for measuring filovirus infectivity*. Journal of Virological Methods, 2013. **193**(2): p. 565-571.
26. Charm, S.E. and B.L. Wong, *Enzyme inactivation with shearing*. Biotechnology and Bioengineering, 1970. **12**(6): p. 1103-1109.
27. Tramper, J., et al., *Shear sensitivity of insect cells in suspension*. Enzyme and Microbial Technology, 1986. **8**(1): p. 33-36.
28. Vickroy, B., K. Lorenz, and W. Kelly, *Modeling Shear Damage to Suspended CHO Cells during Cross-Flow Filtration*. Biotechnology Progress, 2007. **23**(1): p. 194-199.
29. Sánchez Pérez, J.A., et al., *Shear rate in stirred tank and bubble column bioreactors*. Chemical Engineering Journal, 2006. **124**(1): p. 1-5.
30. B. Robertson, J.J.U., *Measurement of shear rate on an agitator in a fermentation broth*. Biotechnology Processes, 1987. **Scale-up and Mixing, American Institute of Chemical Engineers, New York, 1987, pp. 72–81**.
31. Murhammer David, W. and F. Goochee Charles, *Sparged Animal Cell Bioreactors: Mechanism of Cell Damage and Pluronic F-68 Protection*. Biotechnology Progress, 1990. **6**(5): p. 391-397.
32. Maranga, L., et al., *Scale-up of virus-like particles production: effects of sparging, agitation and bioreactor scale on cell growth, infection kinetics and productivity*. Journal of Biotechnology, 2004. **107**(1): p. 55-64.

Figures

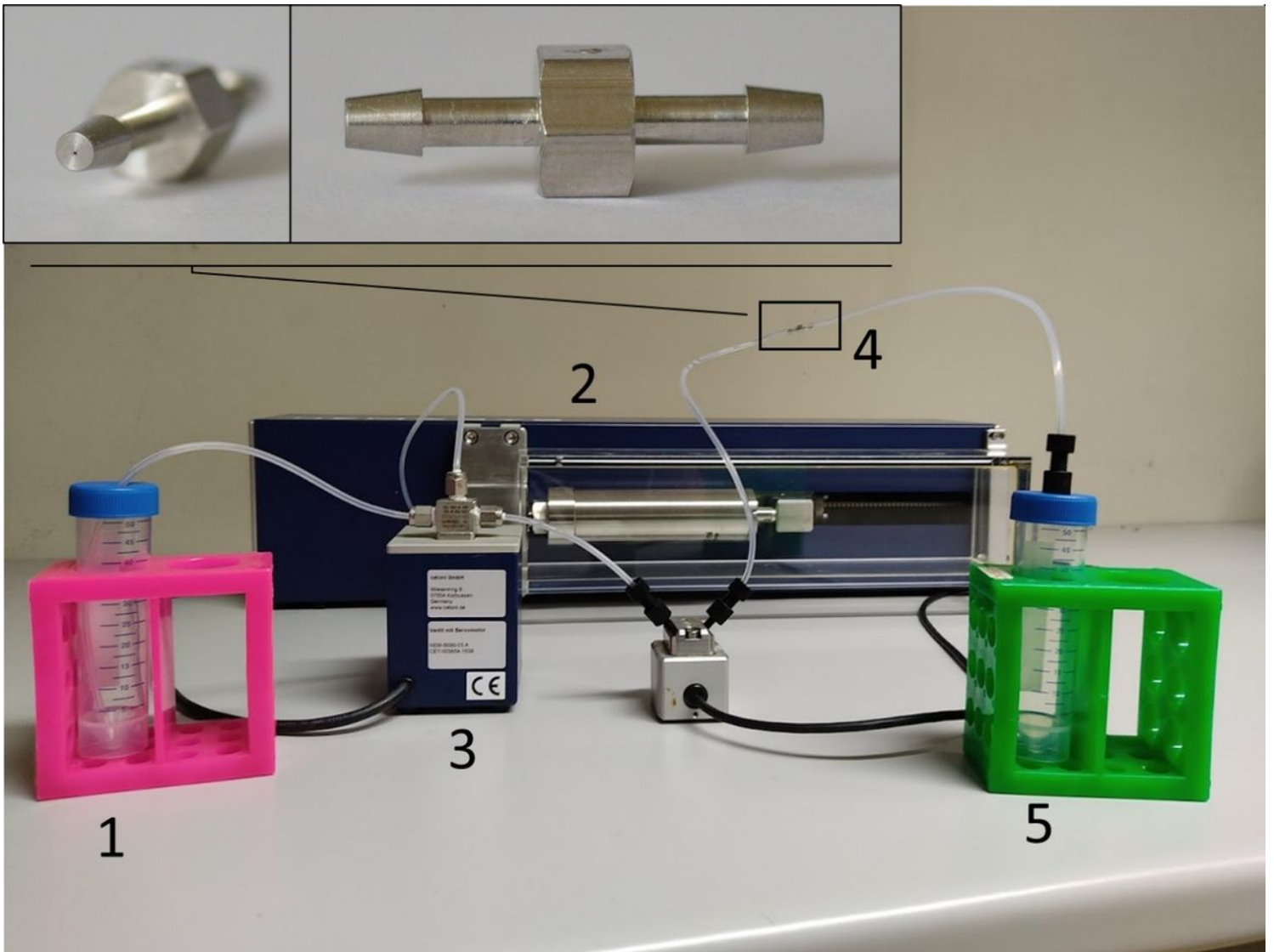


Figure 1

Photograph of the cell stressing set-up. (1) Sample reservoir, (2) syringe pump, (3) 2-way valve, (4) orifice, (5) sample collector. In the top left corner, the two insets display magnifications of the orifice (4).

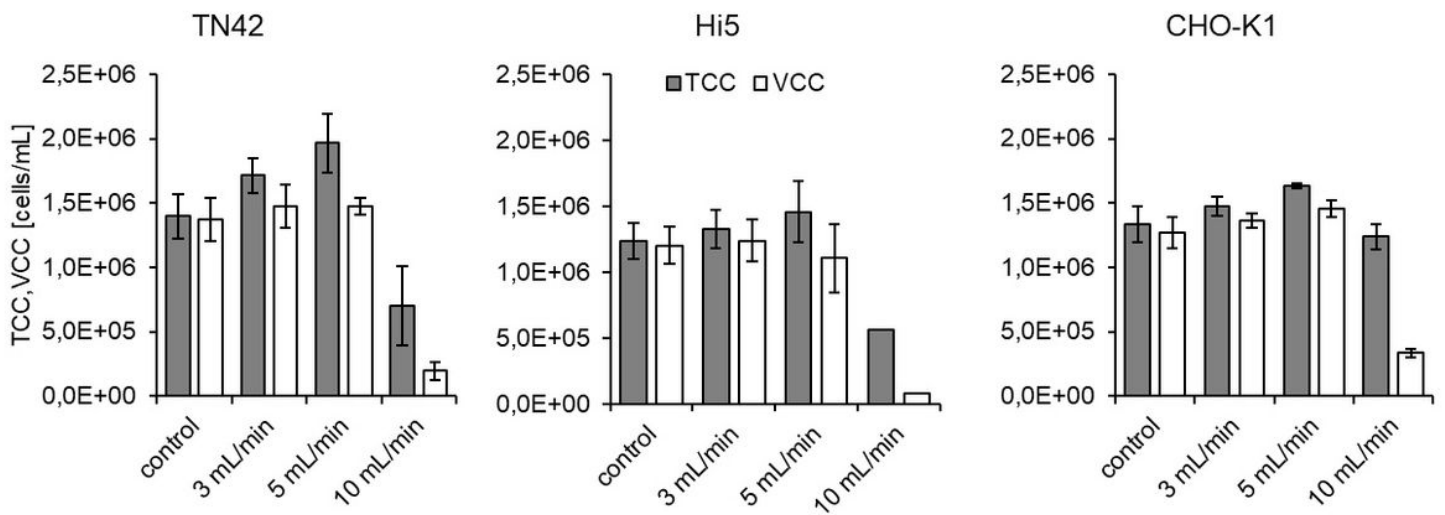


Figure 2

Total and viable cell counts after treatment with the shear device. Shear was measured at different flow rates for (left) TN42, (center) Hi5, and (right) CHO-K1 cells. Each run was performed in triplicate, except the Hi5 experiment (center) run at 10-mL/min.

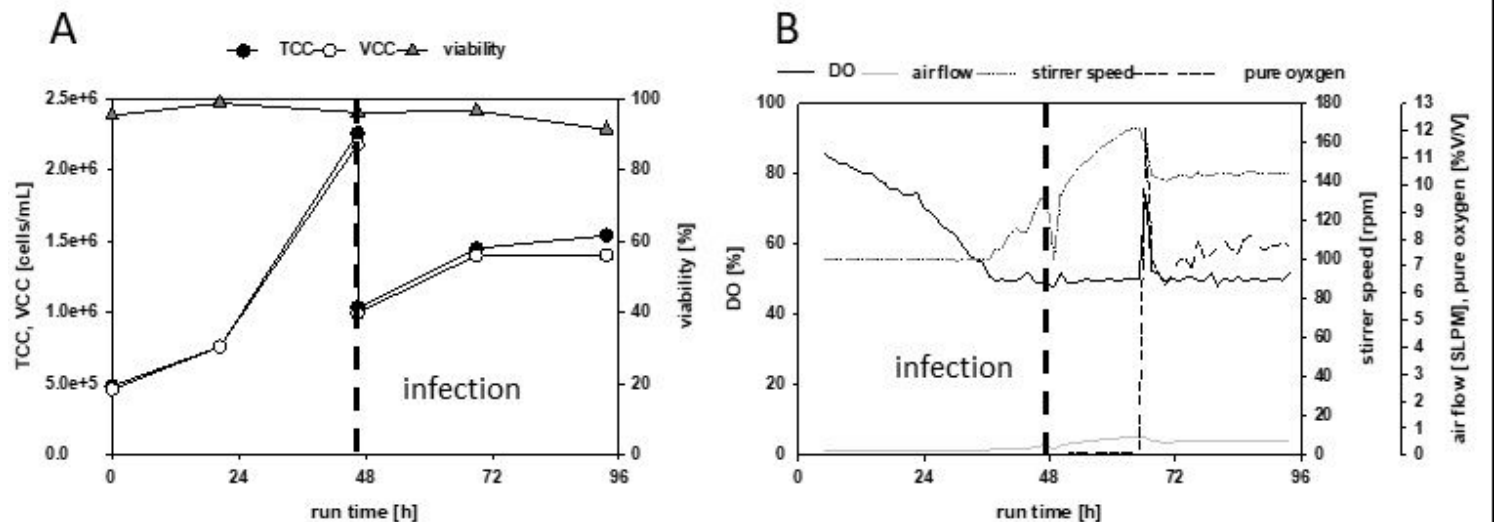


Figure 3

Reference process with TN42 insect cells. (A) Counts of total cells (TCC, filled symbols) and viable cells (VCC, open symbols), before and after infection (dashed line), and cell viability (triangles) over the course of the cultivation. (B) Trends are shown for the dissolved oxygen (DO)-level, the airflow, the stirrer speed, and the percentage of pure oxygen in the airflow. The time point of infection is indicated by the vertical bold dashed line.

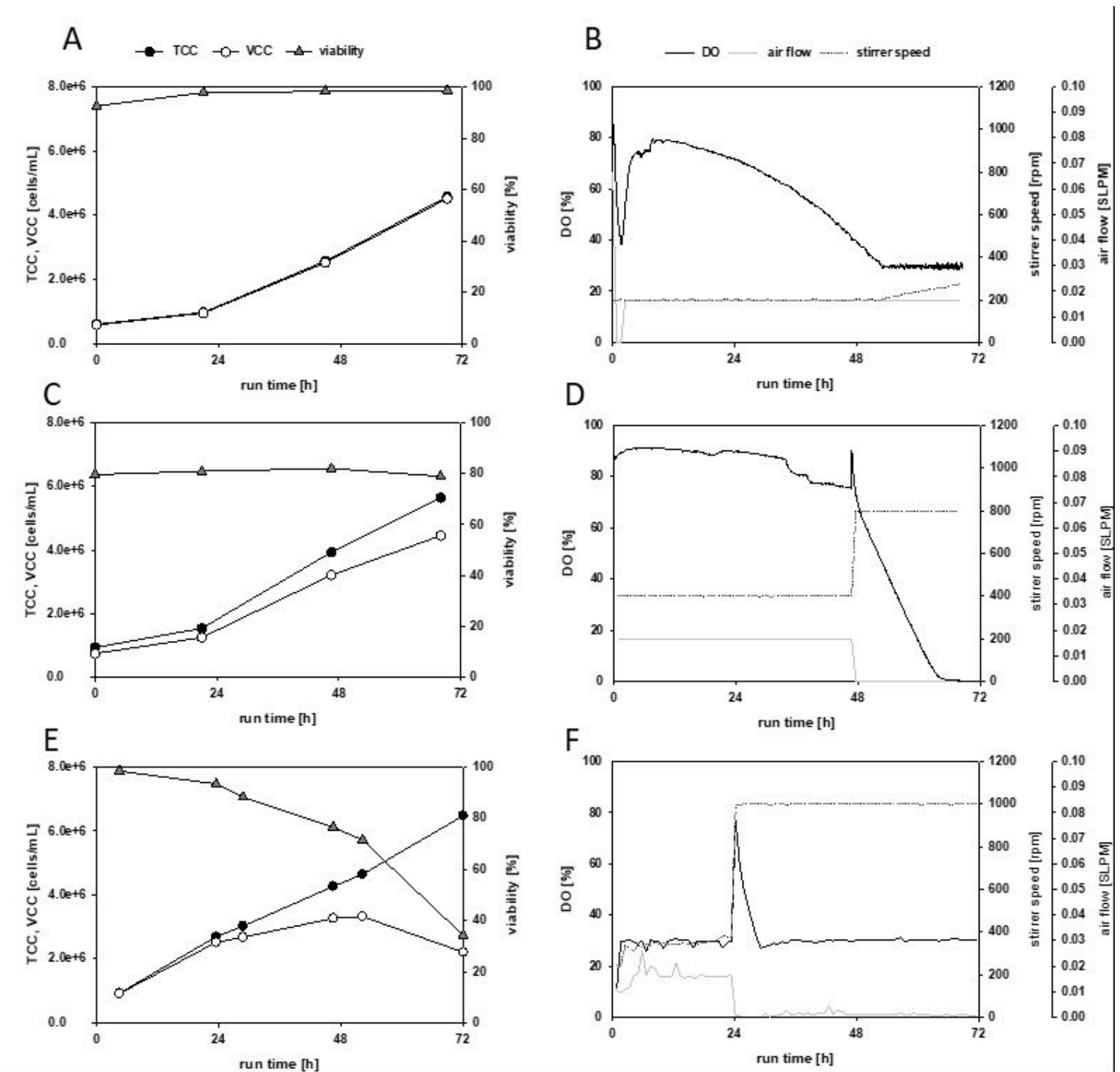


Figure 4

Batch fermentation of TN42 insect cells in a microbial bioreactor, at high stirring speeds. Bioreactors were equipped with either (A,B) one Rushton impeller or (C-F) 3 levels of impellers. (Left column) Viability (triangles), and counts of total cells (TCC, filled circles) and viable cells (VCC, open circles) in the batch cultivation; (right column) the corresponding dissolved oxygen (DO, black solid line), stirring speed (dotted line), and air flow (grey solid line). Stirring speeds were (A,B) 200 rpm, incrementally increased to 270 rpm; (C,D) 400 rpm, stepped to 800 rpm at 48 h; (E,F) 400 rpm, stepped to 1000 rpm at 24 h

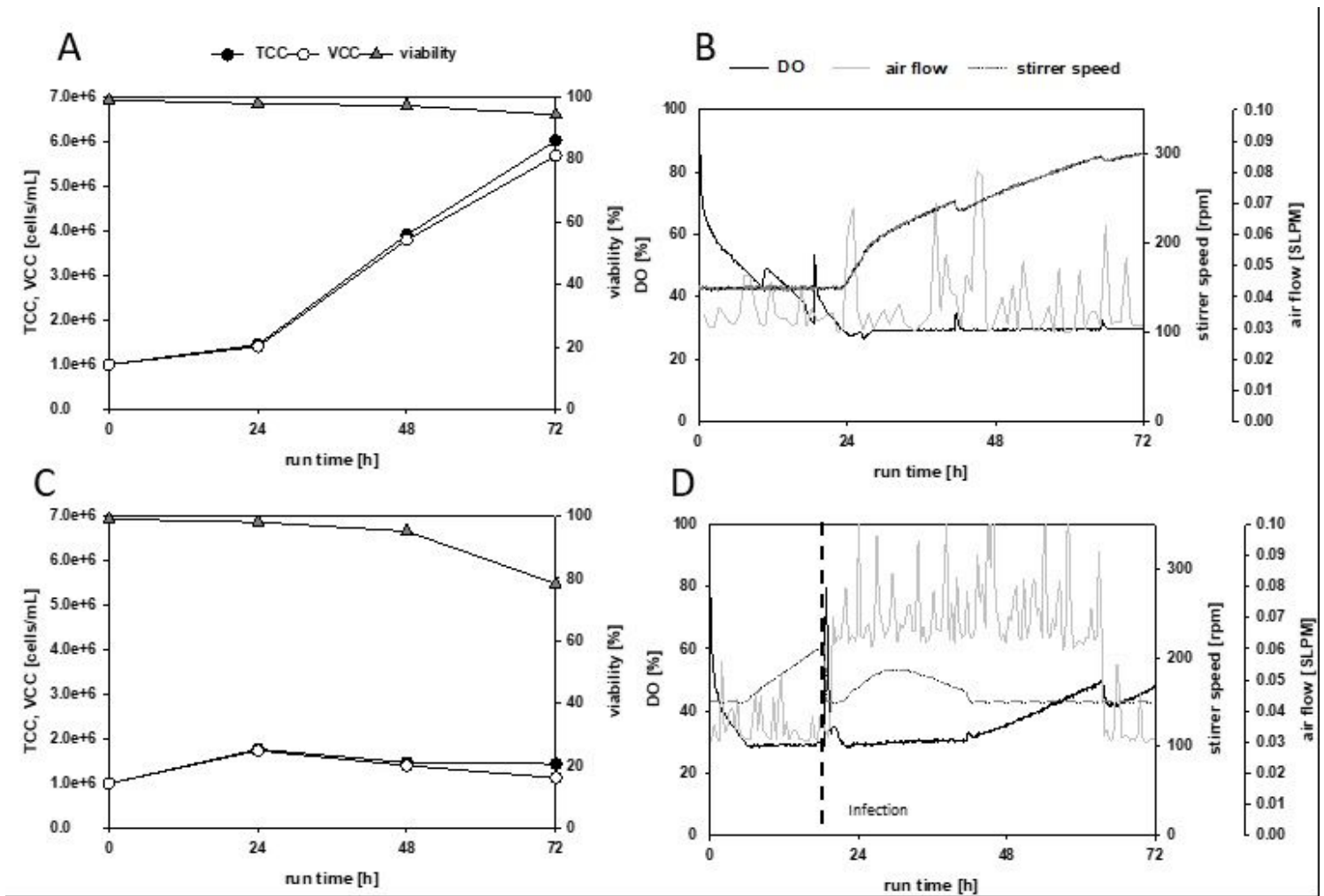


Figure 5

Testing a new control strategy on two cultivations of TN42 insect cells. The controller was tested on (A,B) an uninfected batch cultivation, and (C,D) an infected batch process. In both cases, the starting stirring speeds were 150 rpm, and the controller increased or decreased the speed to maintain the DO at 30%. (A,C) Counts of total (TCC, filled circles) and viable (VCC, open circles) cells, and cell viability (triangles) over the course of the batch cultivation. (B,D) Dissolved oxygen (DO, solid black line), air flow (solid grey line), and agitation speed (dotted line). The vertical line in Figure D indicates the time of infection.

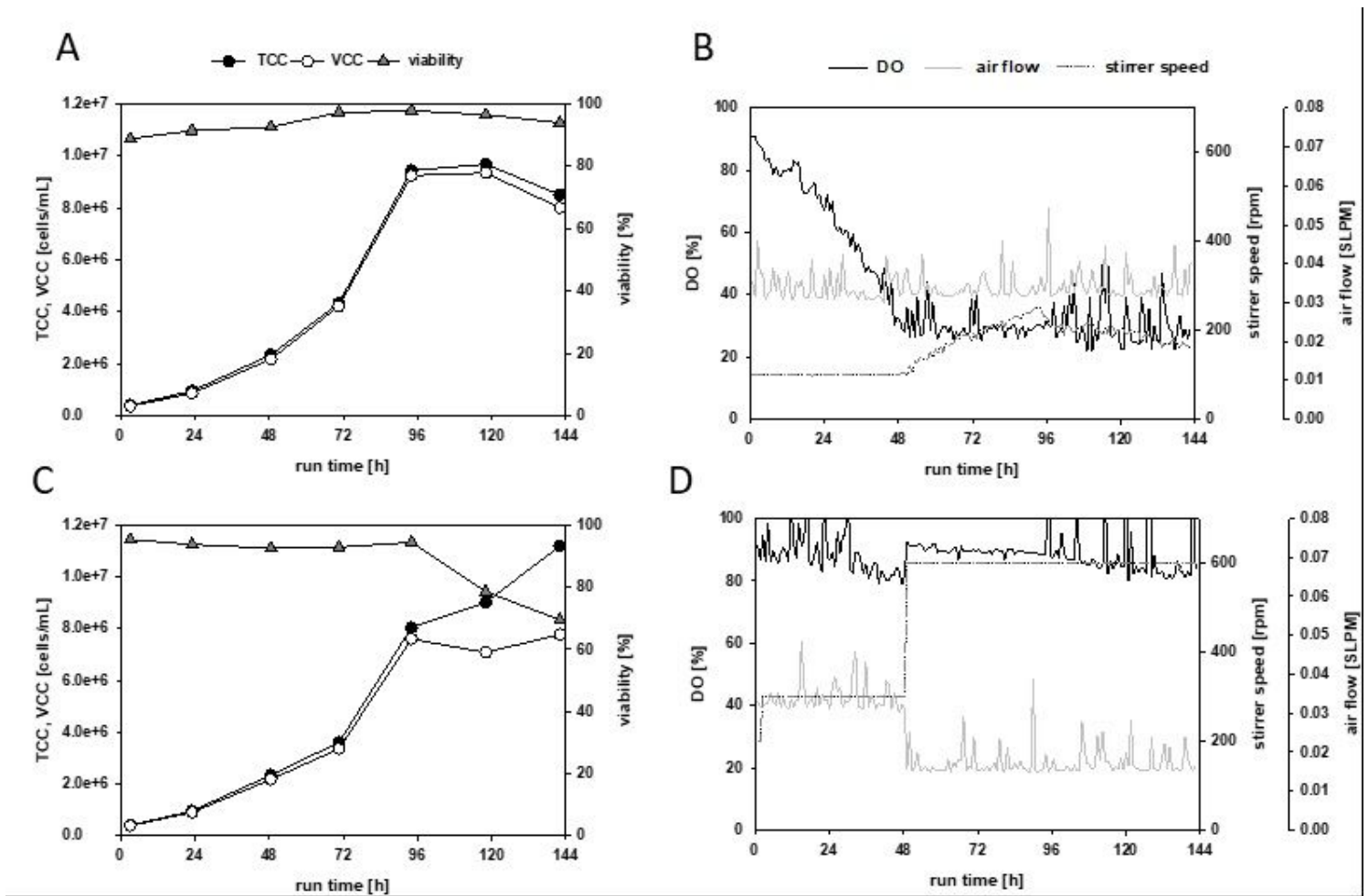


Figure 6

The impact of a high stirring speed tested by comparing two cultivations of CHO cells in microbial bioreactors, at different stirring speeds. (A,B) A standard batch cultivation with a low stirring speed (100 rpm); (C,D) a batch process with a high stirring speed (300 stepped to 600 rpm). (Left column) Viability (triangles), and counts of total cells (TCC, filled circles) and viable cells (VCC, open circles) in the batch cultivation; (right column) the corresponding dissolved oxygen (DO, black solid line), stirring speed (dotted line), and air flow (solid grey line)